

ANALYSIS OF CARBON FIBER SHEET RETROFITTED RC BRIDGE COLUMNS

Richelle Gallardo Zafra¹ and Kazuhiko Kawashima²

¹Assistant Professor, Dept. of Civil Engineering, University of the Philippines Los Baños, Philippines

²Professor, Dept. of Civil Engineering, Tokyo Institute of Technology, Japan

Email: rgzafra@gmail.com, kawashima.k.ae@m.titech.ac.jp

ABSTRACT:

Experimental studies were conducted by some researchers to investigate the cyclic performance of CFS-retrofitted columns; however there is a need to develop analytical methods which can simulate its hysteretic response. This study presents an analysis of the hysteretic behavior of CFS-retrofitted reinforced concrete circular columns. Fiber element analysis was conducted based on cyclic constitutive models of longitudinal reinforcement and concrete confined by both CFS and tie reinforcement. The analysis was verified based on available cyclic test data and analysis provides good agreement with the experimental results. Using the fiber element analysis, the effect of CFS retrofit on the seismic response of a prototype pier was also clarified.

KEYWORDS: Bridge columns, reinforced concrete, carbon-fiber sheet, non-linear analysis, cyclic response

1. INTRODUCTION

Under strong seismic excitations, reinforced concrete bridge columns designed using earlier codes are commonly deficient in flexural ductility, shear strength and flexural strength. Various retrofitting techniques have been developed and the use of fiber-reinforced plastic/polymer (FRP) composite jackets has been widely applied to provide lateral confinement for enhanced strength and ductility. Among the FRP used for the retrofit of reinforced concrete columns, carbon fiber sheets (CFS) are widely used due to its high elastic modulus and tensile strength, the highest among the FRP composites.

Several constitutive models governing the behavior of CFS-confined concrete under monotonic loading have been developed (Spoelstra and Monti 1999, Kawashima *et al.* 2000, Xiao and Wu 2000). On the other hand, very limited studies are available to assess its cyclic response. Kawashima *et al.* (2000), Chang *et al.* (2004), Haroun and Elsanadedy (2005), among others have experimentally investigated the performance of CFS-wrapped reinforced concrete bridge columns under simulated seismic actions. Their results showed that the retrofitted columns had improved seismic performance.

Although experimental studies were conducted to investigate the cyclic performance of CFS-retrofitted columns, there is a need to develop an analytical model which can simulate the experimental results. Also, development of an analytical model that can represent inelastic stiffness and energy-absorbing characteristics of the composite column is necessary for detailed analysis of such systems for practical applications such as in nonlinear static and dynamic analysis.

This paper presents an analysis of the hysteretic behavior of CFS-retrofitted RC columns under an applied axial force and cyclic loading conditions that induce uniaxial bending using the fiber element model. The experimental data obtained by Kawashima *et al.* (2000) were used to validate the model. The components of the model, validation of the model, results and conclusions are discussed in detail in the following sections.

2. EXPERIMENTAL TEST AND ANALYTICAL MODEL

Cyclic Loading Test by Kawashima et al. (2000)

Kawashima *et al.* (2000) tested in cyclic loading six reinforced concrete column specimens 400mm in diameter and 1350mm in effective height. Figure 1 shows the specimen geometry and reinforcement details. Tables 1 and 2 summarize column section properties and CFS material properties, respectively.

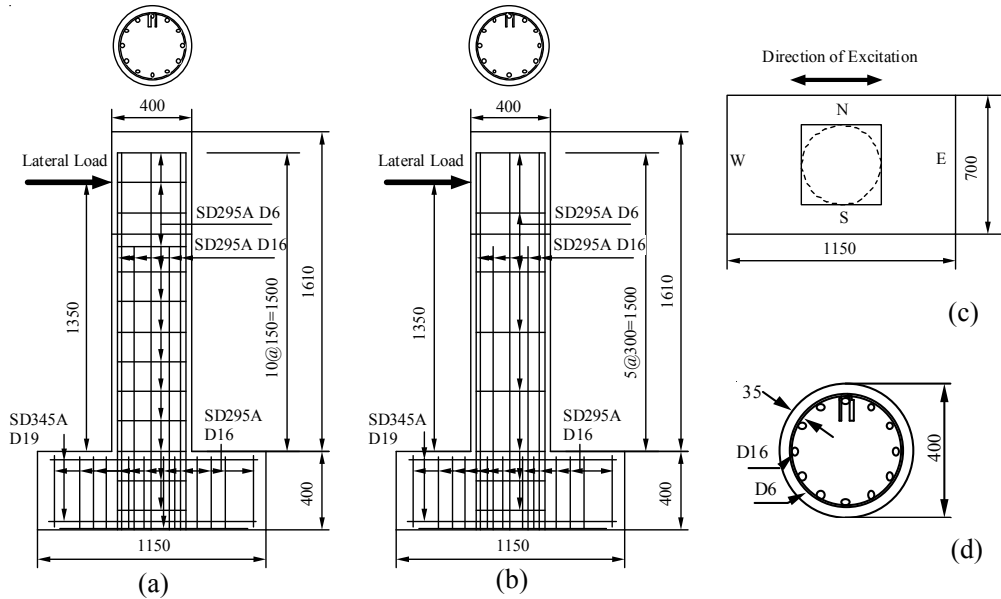


Figure 1. Column specimens for cyclic loading test: (a) A1~A3 specimen, (b) B1~B3 specimen, (c) top view, and (d) section (Kawashima *et al.*, 2000)

Table 1. Column specimen properties for cyclic loading test (Kawashima *et al.* 2000)

Specimens	Series A			Series B		
	A1	A2	A3	B1	B2	B3
Diameter (mm)	400					
Effective Height (mm)	1350					
Shear-Span Ratio	3.375					
Axial Reinforcement Ratio (%)	1.89					
Tie Spacing (mm)	150	150	150	300	300	300
Tie Reinforcement Ratio, ρ_s (%)	0.256	0.256	0.256	0.128	0.128	0.128
CFS Ratio, ρ_{CFS} (%)	0	0.111	0.222	0	0.111	0.222
Concrete Strength (MPa)	30.0	30.0	27.5	30.0	30.0	27.5

Table 2. Properties of CFS used in the experiment (Kawashima *et al.* 2000)

Properties	Nominal	Measured
Amount of CF (g/m ²)	200	200
Thickness of sheet (mm)	0.111	0.111
Tensile Strength (MPa)	3400	4476
Elastic Modulus (GPa)	230	266
Rupture Strain (%)	1.50	1.63

As summarized in Table 1, the specimens were grouped into A and B series where each series consists of three specimens each; one was as-built while the second and third were wrapped laterally by CFS with single layer and two layers, respectively. CFS ratio was 0.111% and 0.222% when the columns were wrapped by single layer and two layers, respectively. The specimens were reinforced in the transverse direction by 6mm deformed bars having yield strength of 363MPa (SD295). The tie reinforcement ratio was 0.256% (150mm-spacing) for the A-series and 0.128% (300mm-spacing) for the B-series. All specimens were reinforced in the longitudinal direction by 16mm deformed bars having yield strength of 374MPa (SD295). Under a constant compression of 185 KN, the piers were loaded in the lateral direction with a displacement increment of a half drift. At each increment, three cyclic loads were applied. The columns were designed such that they fail in flexure.

Analytical Model

To simulate the experimental behavior of the columns, the analytical model consists of a beam element and a fiber element. The fiber element represents the plastic hinge region and its length was assumed to be one-half of the column diameter based on the seismic design requirements of the 2002 Japanese Specifications for Highway Bridges. A rotational spring at the bottom of the column represents the longitudinal bar pull-out from the footing.

In this study, the constitutive relation of concrete confined by ties follows the model of Hoshikuma *et al.* (1997). For concrete confined by CFS and ties, stress-strain relation was based on Kawashima *et al.* model (2000). To describe the hysteretic behavior of the concrete stress-strain relation, Sakai and Kawashima (2006) unloading and reloading model for concrete confined by ties was implemented. This model includes the effect of repeated unloading/reloading cycles, which is characteristic of seismic forces. The modified Menegotto-Pinto model (Menegotto and Pinto, 1973) was used to idealize the stress vs. strain relation of the longitudinal reinforcements. The effect of local buckling and rupture of longitudinal reinforcing bars are neglected.

3. MODEL VALIDATION

Experimental Behavior

As reported by Kawashima *et al.* (2000), for as-built columns A1 and B1 the cover concrete spalled-off 200mm and 300mm from the bottom, respectively. Buckling of main bars occurred at 3.5% drift for A1 and 3.0% drift for B1. In contrast to the as-built columns, spalling-off of cover concrete for the retrofitted columns A2, A3, B2, and B3 was well prevented by the CFS. Rupture of CFS was not observed in all the retrofitted specimens; however, flexural cracks developed on the column specimens. As the loading displacement increased, the crack widths also increased. For example, in columns A2 and B2, at 3.0% drift, cracks occurred at 150 mm and 300 mm from the base. Afterwards, numerous cracks gradually developed within the range from the base up to a height of 200 mm. At 5.5% drift, a large crack occurred in the CFS at the bottom.

Figure 2 shows the lateral force vs. lateral displacement hysteresis of the columns under cyclic loading obtained from the experiment. For the as-built columns, it is noted that a sudden deterioration of the restoring force occurred at 3.5% drift for A1 and 3.0% drift for B1. This can be attributed to the spalling-off of cover concrete which induced the buckling of the main bars at these drift ratios. The restoring force decreased to less than 50% of the maximum at 3.5% drift in both A1 and B1. Compared to the as-built columns, the retrofitted columns demonstrated a stable response in the entire loading displacement range tested as a result of CFS confinement. Deterioration of the restoring force occurred at 5.5% drift for both A2 and B2 and 5% drift for both A3 and B3.

To determine the effect of the CFS for retrofit, CFS volumetric ratio was varied for different tie reinforcement ratios. It can be seen in Figures 3(a) and 3(b) that increased flexural strength and ductility is attained with increased volumetric ratio of CFS. However, the flexural strength and ductility of column confined by one

layer of CFS ($\rho_{CF} = 0.111\%$) was larger compared to the column confined by two layers of CFS ($\rho_{CF} = 0.222\%$).

The effect of increasing tie reinforcement ratio on the hysteretic response of CFS-retrofitted columns is shown in Figures 4(a) and 4(b). Since low tie reinforcement ratios were considered, not much difference was observed in the response.

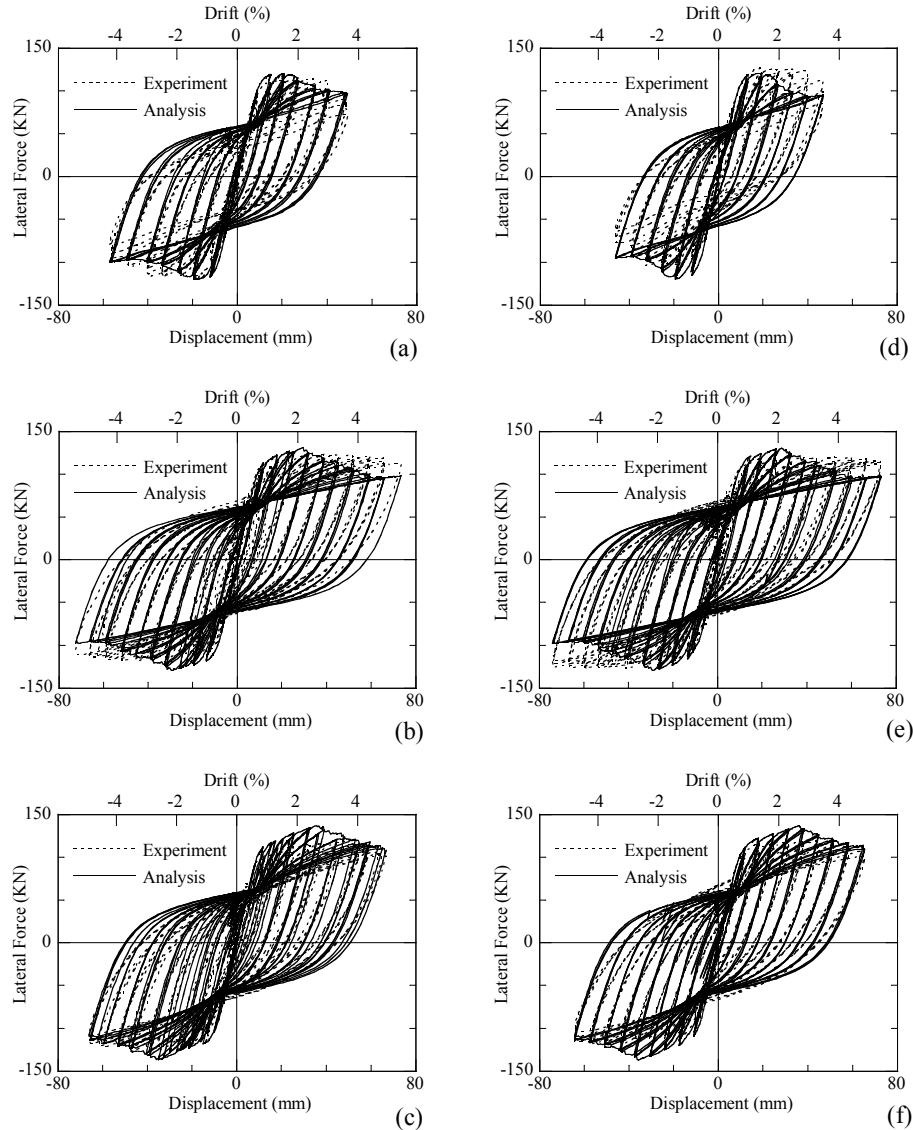


Figure 2. Comparison of lateral force vs. lateral displacement hysteresses between experiment and analysis: (a) A1, (b) A2, (c) A3, (d) B1, (e) B2, and (f) B3

Analytical Correlation

Figure 2 shows the analytical hysteresis in comparison with the experimental hysteresis. In general, there is a very good agreement between the analytical and experimental results. In the analysis, deterioration of the restoring force for all column specimens is much earlier compared to the experimental results. For the as-built columns A1 and B1, the restoring force decreased at 2.0% drift while for the retrofitted columns, deterioration

occurred at 2.5% drift for columns A2 and B2 and 3.0% drift for columns A3 and B3. It can be observed from Figure 2 that unloading and reloading hysteresis of the experimental results is adequately simulated by the analysis.

Similar to the experiment, analysis shows that when CFS volumetric ratio increases, flexural strength and ductility also increases as shown in Figures 3(c) and 3(d). When tie reinforcement ratio is increased, not much difference is observed on the hysteretic response of CFS-retrofitted columns for low tie reinforcement ratios as shown in Figures 4(c) and 4(d).

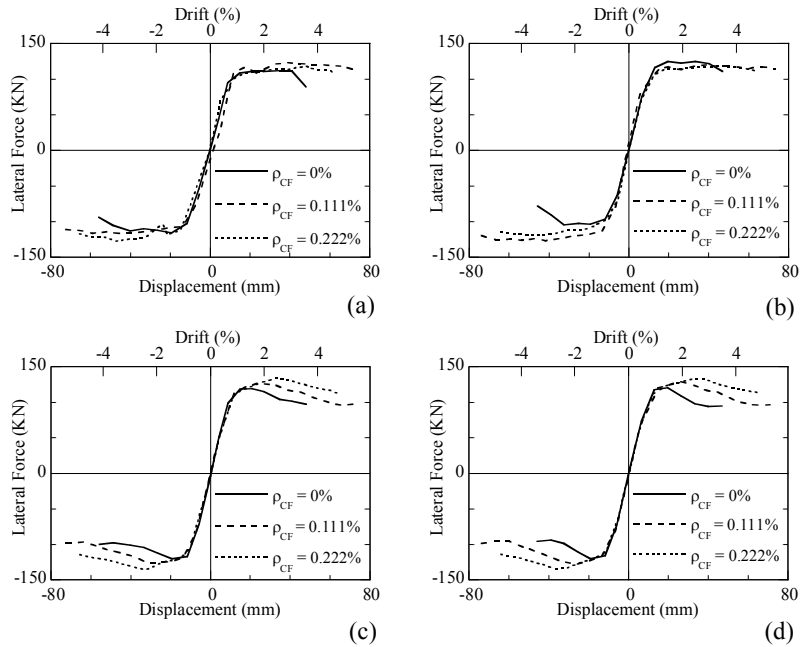


Figure 3. Effect of CFS quantity: (a) experiment ($\rho_s = 0.256\%$), (b) experiment ($\rho_s = 0.128\%$) (c) analysis ($\rho_s = 0.256\%$) and (d) analysis ($\rho_s = 0.128\%$)

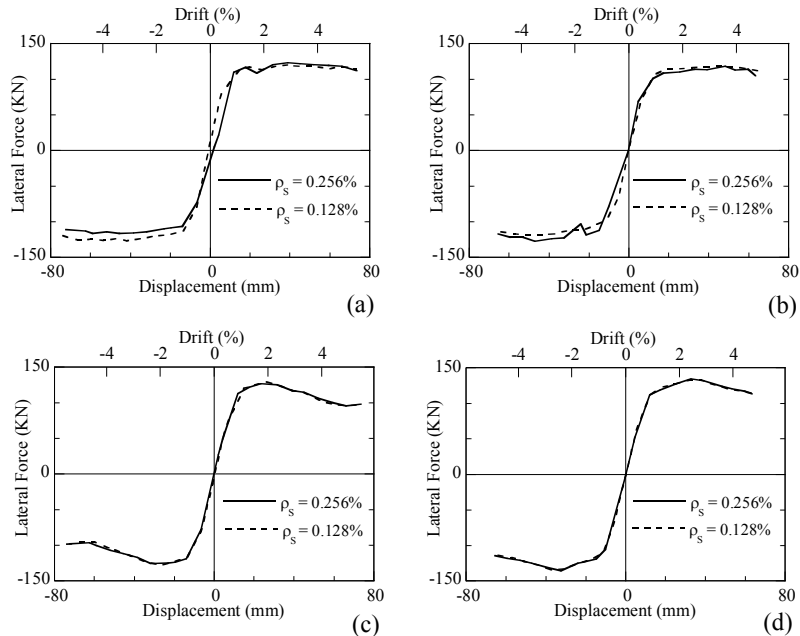


Figure 4. Effect of tie reinforcement quantity: (a) experiment ($\rho_{CF} = 0.111\%$), (b) experiment ($\rho_{CF} = 0.222\%$), (c) analysis ($\rho_{CF} = 0.111\%$), (d) analysis ($\rho_{CF} = 0.222\%$)

4. APPLICATION TO PROTOTYPE PIERS

Pier Analyzed

The analytical procedure earlier described was used to analyze a prototype pier. The pier considered is part of the E-Defense Large Shake Table Test of bridges based on NEES and E-Defense collaboration. The pier is a 7.5-m tall circular reinforced concrete column with a diameter of 1.8 m supported by a 6 m by 6 m by 2 m thick footing (Figure 5a). The pier supports an inertia mass of 170 tons. It is a typical column built in the 1970s to 1980s designed based on the seismic coefficient method (0.23 horizontal and 0.11 vertical seismic coefficients) and allowable stress design approach. The design compressive strength of concrete is 27 MPa. Eighty-29 mm diameter deformed bars with 295 MPa nominal strength (SD295) are used as longitudinal reinforcement. The same class 13 mm deformed bars are used as ties spaced 300 mm along the column axis. The longitudinal reinforcement ratio and the tie volumetric ratio are 2.02% and 0.104%, respectively.

The footing was assumed to be supported by cast-in-place reinforced concrete piles. The soil condition was assumed to consist of sand and gravel and is classified as Type II ground condition (moderate ground condition) based on the current 2002 Japan Road Association - Specifications for Highway Bridges.

The effect of CFS retrofit on the seismic response of the pier was also investigated analytically. The pier wrapped laterally by CFS with single layer and three layers was considered. Corresponding CFS ratio was 0.027% and 0.082%, respectively. CFS was assumed to be wrapped along the entire height of the pier. CFS material properties, previously shown in Table 2, were used.

Analytical Model and Ground Motions

The pier was idealised by a fiber element and linear beam elements (Figure 5d). The length of the fiber element was assumed to be one half of the pier diameter. The foundation was assumed to be rigid and its effect was idealized by a set of equivalent linear springs. Near-field ground motion recorded at JMA Kobe Observatory in the 1995 Kobe, Japan earthquake was used as the input ground motion. The NS component was applied to the pier in the longitudinal (NS) direction in the unilateral excitation while the NS, EW, and UD components of the ground acceleration were applied to the pier in the longitudinal (NS), transverse (EW), and vertical (UD) directions, respectively, in the tri-axial excitation. Damping ratio of 2% was assumed in the numerical integration of the equations of motion.

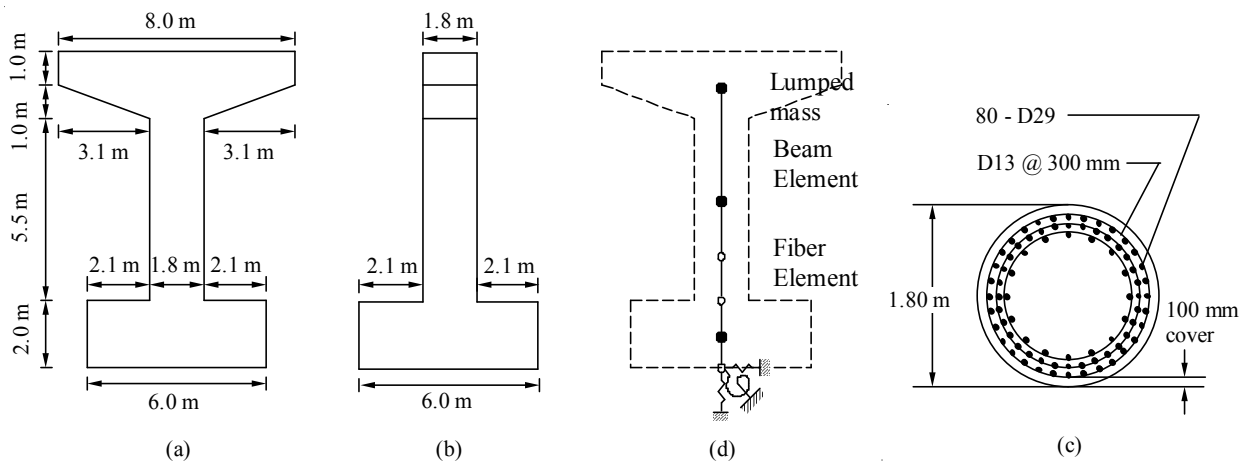


Figure 5. Prototype pier: (a) front view; (b) side view; (c) cross-section at the base of pier; (d) analytical model.

Dynamic Response of As-Built Pier and CFS-Retrofitted Pier

Figure 6 shows the response displacement and the lateral force-lateral displacement hysteresis at the center of gravity of the top mass of the as-built pier in the NS direction under the unilateral excitation. The analytical results show that maximum displacement of 123 mm was incurred. The maximum lateral force was 2632 KN in the positive direction and 1488 KN in the negative direction.

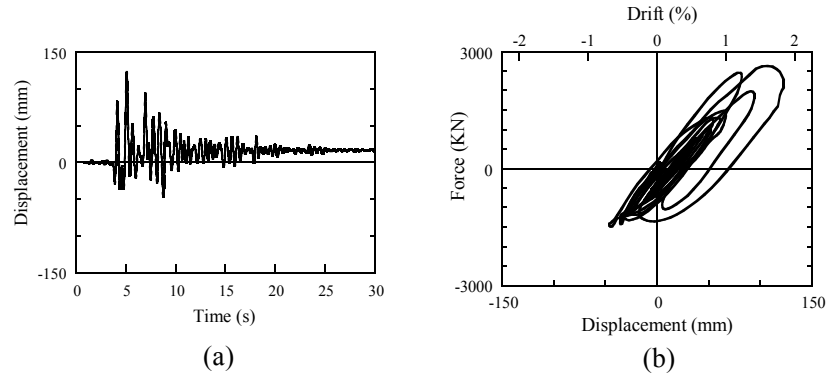


Figure 6. Response of as-built pier under unilateral excitation: (a) displacement response at center of gravity of top mass; (b) lateral force vs. lateral displacement hysteresis.

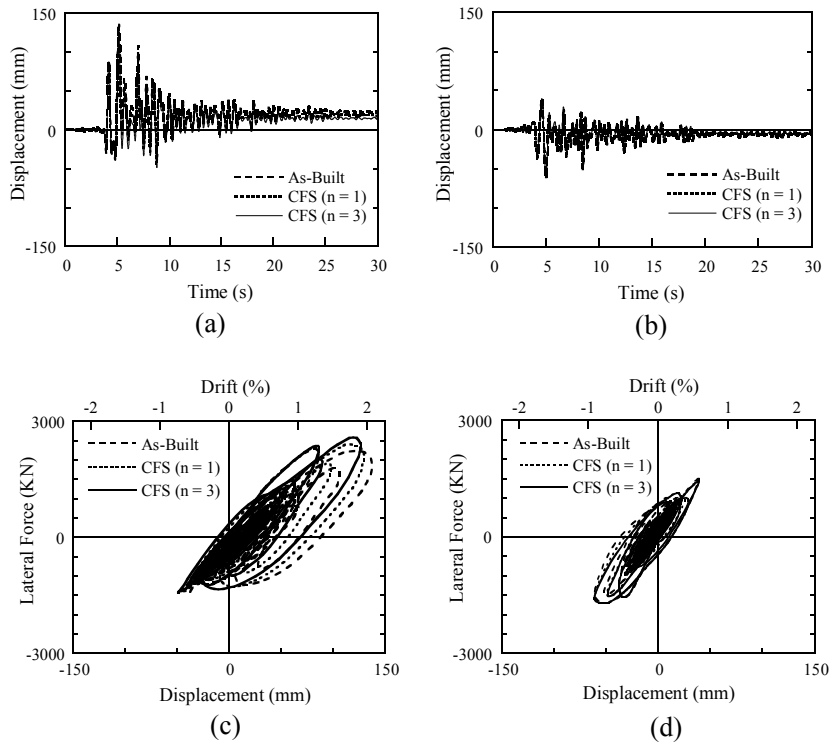


Figure 7. Response of as-built pier under tri-axial excitation: (a) displacement response (NS); (b) displacement response (EW); (c) lateral force-lateral displacement hysteresis (NS) and (d) lateral force-lateral displacement hysteresis (EW)

Figure 7 compares the response displacements and the lateral force-lateral displacement hystereses of the as-built pier and CFS-retrofitted pier under the tri-axial excitation. For the as-built pier, it is important to note that

the maximum lateral force in the NS direction was 2255 KN which was 17% smaller than that under the unilateral excitation. The maximum lateral force in the EW direction was 1760 KN. The maximum displacement in the NS direction was 136 mm, which was 10% larger compared to that under unilateral excitation. The maximum displacement in the EW direction was 62 mm.

For the retrofitted pier, the lateral force in the NS and EW direction increased as the thickness (or the number of sheets) of CFS increased. CFS retrofit increased the flexural strength of the as-built column. On the other hand, the displacement response of retrofitted piers in both the NS and EW direction decreased as the thickness (or the number of sheets) of CFS increased. Enhancement of the flexural capacity of the pier was in favor of mitigating the residual displacement after an earthquake.

4. CONCLUSIONS

The nonlinear response of scaled CFS-retrofitted circular columns under unilateral cyclic loading was simulated using the fiber element analysis. Based on the results presented, the following conclusions can be made:

- i. The fiber element analysis which is based on cyclic constitutive models of longitudinal reinforcement and concrete confined by both CFS and ties provides good numerical simulation of the experimental results.
- ii. The hysteretic response of as-built columns can be enhanced by CFS jacketing which is effective at increasing lateral confinement, allowing an increase in strength and ductile behavior.
- iii. Simulation of the 7.5 m tall pier under a large earthquake shows that CFS retrofit increases the flexural strength of the as-built pier while limiting its displacement.

REFERENCES

- Chang, S., Li, Y. and Loh, C. (2004) Experimental study of seismic behaviors of as-built and carbon fiber reinforced plastics repaired reinforced concrete bridge columns, *Journal of Bridge Engineering* **9(4)**, 391-402.
- Haroun, M. and Elsanadedy, H. (2005) Fiber-reinforced plastic jackets for ductility enhancement of reinforced concrete bridge columns with poor lap-splice detailing, *Journal of Bridge Engineering* **10(6)**, 749-757.
- Hoshikuma, J., Kawashima, K., Nagaya, K. and Taylor, A. (1997) Stress-strain model for confined reinforced concrete in bridge piers, *Journal of Structural Engineering* **123(5)**, 624-633.
- Japan Road Association (2002) Specifications for Highway Bridges - Part V Seismic Design Maruzen, Tokyo.
- Kawashima, K., Hosotani, M. and Yoneda, K. (2000) Carbon fiber sheet retrofit of reinforced concrete bridge piers. **Proc. of the International Workshop on Annual Commemoration of Chi-Chi Earthquake**, Vol. II-Technical Aspect, National Center for Research on Earthquake Engineering, Taipei, Taiwan, ROC, pp. 124-135.
- Menegotto, M. and Pinto, P. (1973) Method of analysis for cyclically loaded reinforced concrete plane frames including changes in geometry and non-elastic behavior of elements under combined normal force and bending. **Proc. of IABSE Symposium on Resistance and Ultimate Deformability of Structures Acted on by Well Defined Repeated Loads**, Lisbon, pp. 15-22.
- Sakai, J. and Kawashima, K. (2006) Unloading and reloading stress-strain model for confined concrete, *Journal of Structural Engineering* **132(1)**, 112-122.
- Spoelstra, M. and Monti, G. (1999) FRP-confined concrete model, *Journal of Composites for Construction* **3(3)**, 143-150.
- Xiao, Y. and Wu, H. (2000) Compressive behavior of concrete confined by carbon fiber composite jackets, *Journal of Materials in Civil Engineering* **12(2)**, 139-146.